

Electronic Supplementary Information

Fully Automated and High-Fidelity Robotic Platform Enabling Accelerated Discovery of Nanocatalysts

Shin Wook Kang,^{a§} Kyung Hee Oh,^{a§} Kanghoon Yim,^b Sanha Jang,^a Jin Gyu Lee,^a Jung-Il Yang,^a and Ji Chan Park^{a,c}*

^a Clean Fuel Research Laboratory, Korea Institute of Energy Research, Daejeon 34129, Republic of Korea.

^b Energy AI & Computational Science Laboratory, Korea Institute of Energy Research, Daejeon 34129, Republic of Korea.

^c Energy Engineering, University of Science and Technology, Daejeon 34113, Republic of Korea

§ S.W.K. and K.H.O. contributed equally to this work.

*Corresponding Author (email): jcpark@kier.re.kr

Experimental Section

Chemicals. Palladium(II) acetylacetonate ($\text{Pd}(\text{acac})_2$, 99 %), iron(II) acetate ($\text{Fe}(\text{CH}_3\text{CO}_2)_2$, 99 %), activated charcoal (100 mesh), 4-nitrophenol (4-NP, ≥ 97 %), sodium borohydride (NaBH_4 , ≥ 96 %), and various metal precursor salts in Table S1 were purchased from Sigma-Aldrich and used as received. Ethanol (99.9 %) was supplied by Samchun Chemicals. A commercial Pd/C catalyst (Evonik NOBLYST® P1070, 10 wt% Pd) was used as a reference.

Synthesis of R-Pd/AC and M-Pd/AC nanocatalysts. R-Pd/AC was prepared with a nominal Pd loading of 10 wt%. In a 1 mL glass vial, 2.3 mg of $\text{Pd}(\text{acac})_2$ (7.55 μmol) and 7.2 mg of activated charcoal (0.6 mmol) were dispersed in 100 μL of ethanol. For M-Pd/AC variants, the same amounts of $\text{Pd}(\text{acac})_2$ and activated charcoal were first suspended in 50 μL of ethanol. A concentrated stock solution of the additive metal precursor (10 mol% relative to Pd) was prepared by dissolving it in 2.5 mL of ethanol (corresponding to a 50 \times scale). Then, 50 μL of this stock solution was added to the Pd/AC slurry. The resulting mixture was vortexed and sonicated for 30 min to ensure uniform dispersion. All slurries were then transferred to alumina crucibles and reduced under hydrogen flow (200 $\text{mL}\cdot\text{min}^{-1}$) in a tubular furnace. The temperature was ramped to 400 $^\circ\text{C}$ at a rate of 3.75 $^\circ\text{C}\cdot\text{min}^{-1}$, and maintained for 30 min. After cooling under nitrogen, the reduced catalysts were collected for testing.

Scale-up synthesis of Fe-Pd/AC catalyst. Fe-Pd/AC was also synthesized on a larger scale ($\times 139$ batch scale) for extended testing. A total of 1.0 g of activated charcoal (83.3 mmol) and 0.318 g of $\text{Pd}(\text{acac})_2$ (1.04 mmol) were premixed in a high-energy ball mill at 1750 rpm for 5 min using a methacrylate grinding ball. Separately, 18.2 mg of $\text{Fe}(\text{CH}_3\text{COO})_2$ (104.6 μmol , 10 mol% relative to Pd) was dissolved in 13.9 mL of ethanol and added to the solid mixture. After stirring, the slurry was dried at 50 $^\circ\text{C}$ under vacuum for 1 h, followed by reduction at 400 $^\circ\text{C}$ for 30 min under a hydrogen flow. The resulting product was cooled under nitrogen and collected for testing.

Catalyst reaction preparation for robotic evaluation. Twenty-four catalyst samples (R-Pd/AC, commercial Pd/C, and 22 M-Pd/ACs) were each manually weighed to a nominal mass of 8.00 mg into single-use polyethylene bottles using a high-precision microbalance (± 0.005 mg tolerance). For all subsequent kinetic analyses, the nominal target mass was used, as such small deviations were negligible with respect to the calculated catalytic activity. Using an Opentrons OT-2 liquid-handling robot, 1.0 mL of 4-NP stock solution (0.072 M) was dispensed into each bottle (**Movie S4[†]**). The bottles were then placed in a custom-designed shaker jig. An auxiliary robot (Wikata Mirobot), paired with a peristaltic pump, delivered 38 mL of deionized water into each bottle along automated, preprogrammed motion paths (**Movie S5[†]**). The reducing agent solution was prepared by dissolving 1.0 g of NaBH_4 and 2.0 g of NaOH in 125 mL of deionized water, yielding a pH of approximately 12 to ensure reductive stability. The solution was subsequently loaded into a reservoir located on the robotic platform.

Automated UV-Vis measurement protocol. After the experimental conditions are set, robot 1 initiates operation via pre-installed robot control program 1. Following the initial manual setup described above, all subsequent experimental steps were executed automatically without human intervention. Once activated, the robots are automatically synchronized with the controller, initiating all movement sequences, data logging, and process execution without manual intervention. The status of the catalytic reactions and data acquisition is displayed in real time and can also be remotely monitored via a CCTV system. To ensure consistent reaction kinetics and homogeneous dispersion, the system employs controlled orbital shaking at 200 rpm, which is sufficient to achieve uniform mixing without causing liquid overflow from the reaction bottles. In addition, temperature regulation and reaction homogeneity are achieved through the use of custom-designed aluminum heating blocks and integrated thermocouples. These thermally conductive blocks maintain the desired reaction temperature uniformly across all bottles, while orbital shaking further ensures dispersion of reactants and catalysts. Prior to initiating the reaction, the solution inside each bottle was fully equilibrated to the set temperature, and thermocouple-based measurements

confirmed that the reaction temperature remained stable throughout the reaction period due to the feedback-controlled heating system.

To investigate the effect of temperature on catalytic performance, catalysts were tested at 25 °C, 30 °C, and 35 °C using the integrated heating system within the robotic platform. Prior to initiating the catalytic reaction, blank measurements are performed to establish a baseline for UV-Vis absorbance. Robot 1 retrieves a clean UV-Vis cell from the storage rack and sequentially dispenses 1.0 mL of deionized water twice into the cell (total volume: 2.0 mL). The cell is then placed into the spectrometer jig, and a blank scan is conducted using the UV-Vis spectrometer, controlled by robot control program 1. After measurement, the UV-Vis cell used for the blank is automatically discarded and replaced by robot 1. To initiate the reaction, robot 2 (operated by robot control program 2) collects 1.0 mL of NaBH₄ solution using a fresh pipette tip and dispenses it into the designated reaction bottles. The used tip is discarded immediately after injection to prevent contamination. The bottle is then gently shaken to ensure thorough mixing of the reactants. Robot 1 subsequently aspirates 60 µL of the reaction mixture at each predetermined time point (0, 3, 6, and 9 min), transfers the aliquot into a fresh UV-Vis cell prefilled with 2.0 mL of deionized water, thoroughly mixes the contents, and places the cell into the UV-Vis spectrometer. Each time-point measurement is performed on an independently sampled aliquot drawn directly from the ongoing reaction, ensuring accurate tracking of reaction kinetics over time. This fully automated sequence is executed for 24 samples per cycle. Upon completion of each cycle, robot 2 replaces the UV-Vis cell jig and pipette tips to ensure cleanliness and prevent cross-contamination before processing the next batch. All acquired absorbance data were automatically transmitted to the control PC for real-time processing and storage, completing the fully automated catalytic activity screening workflow under the coordination of robot control programs 1 and 2. All robotic components in the automated platform including both commercially available instruments and custom-fabricated parts are summarized in Table S3[†].

Characterization. Transmission electron microscopy (TEM) was performed using a JEOL F200 microscope operated at 200 kV and equipped with an energy-dispersive X-ray spectroscopy (EDS) detector (JED-2300T, JEOL Ltd.). TEM samples were prepared via a conventional drop-casting method, where several drops of the colloidal suspension were deposited onto lacey carbon-coated copper grids (Ted Pella, Inc.) and dried under ambient conditions. X-ray diffraction (XRD) measurements were conducted using a high-power powder diffractometer (Rigaku D/MAX-2500, 18 kW) with Cu K α radiation. Data were collected over a 2θ range of 20–80° with a scanning speed of 3° min⁻¹ and a step size of 0.01°.

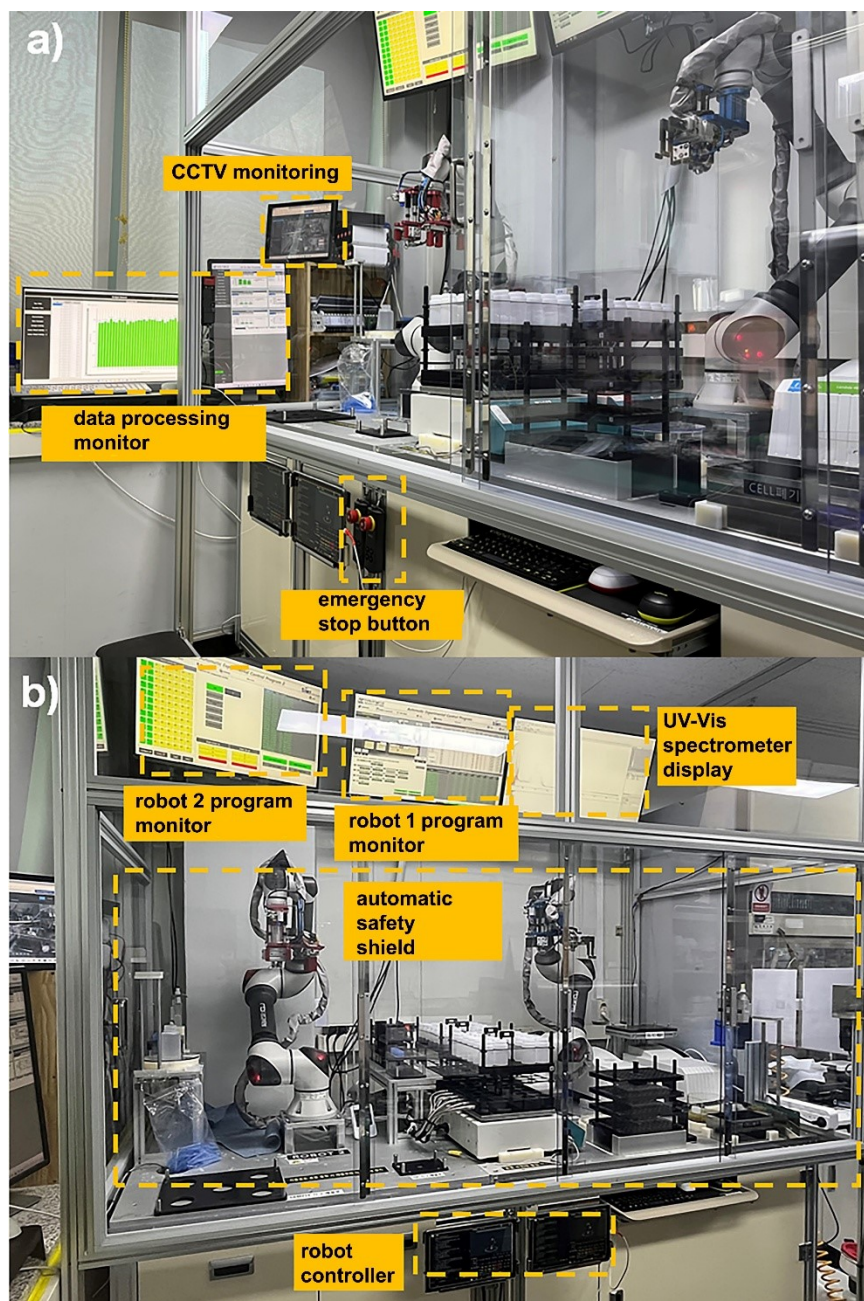


Figure S1. Overview photographs of the automated catalyst evaluation system. (a) Side view of the robot-based high-throughput catalyst screening platform, featuring a CCTV monitoring system, data-processing monitor, emergency stop button, and two coordinated robotic arms operating within a sealed enclosure for operational safety and precision. (b) Front view of the full system layout, showing the two robotic arms controlled via independent program monitors, an integrated UV-Vis spectrometer for in-line kinetic measurements, and a centralized controller module housed beneath the automatic safety shield for coordinated execution of multistep workflows.

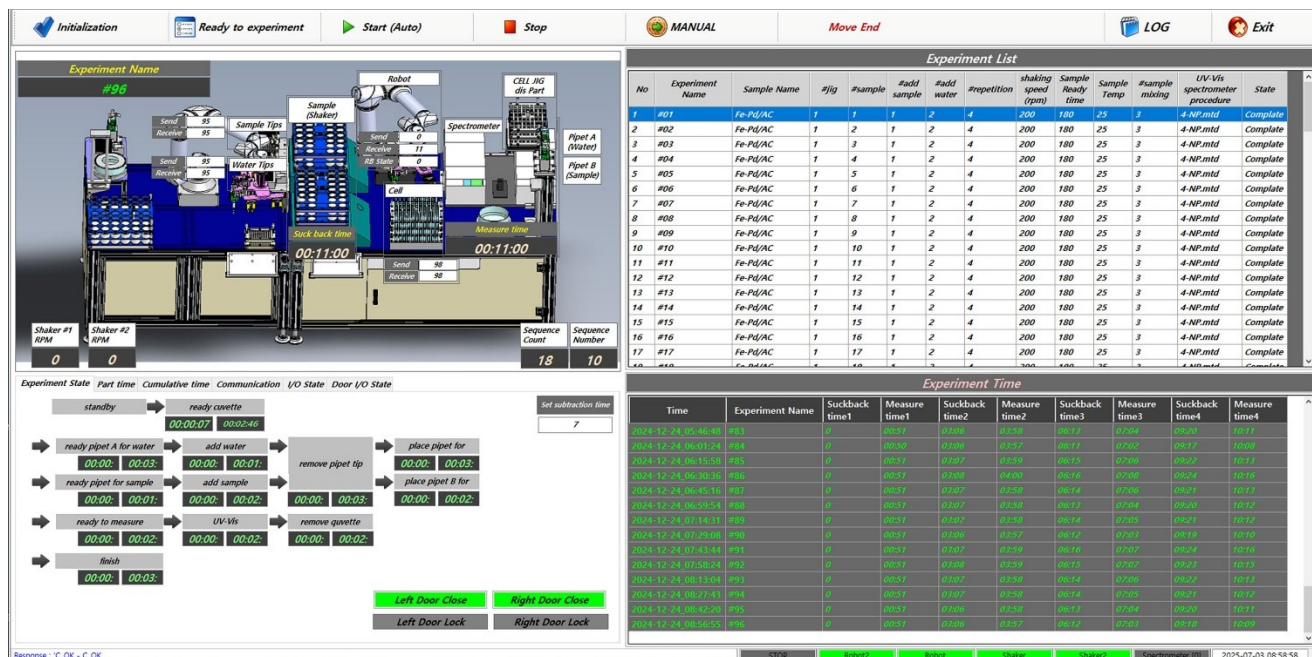


Figure S2. Graphical user interface (GUI) of the automated catalyst screening platform used in robot control program 1. The central interface displays the real-time operation of the system, including robotic handling, pipetting, UV-Vis measurements, and sample shaking. A schematic diagram shows the status of each module, including robot arm positioning, spectrometer timing, shaker speed (RPM), and jig state. The right-side panel lists experimental details for each sample, such as composition, repetition, shaking speed, and UV-Vis procedure. The bottom panel tracks detailed time logs for every measurement and pipetting cycle, enabling transparent, time-resolved diagnostics and process control across all 96 samples. This GUI provides intuitive monitoring and precise control of automated workflows assigned to robot program 1.

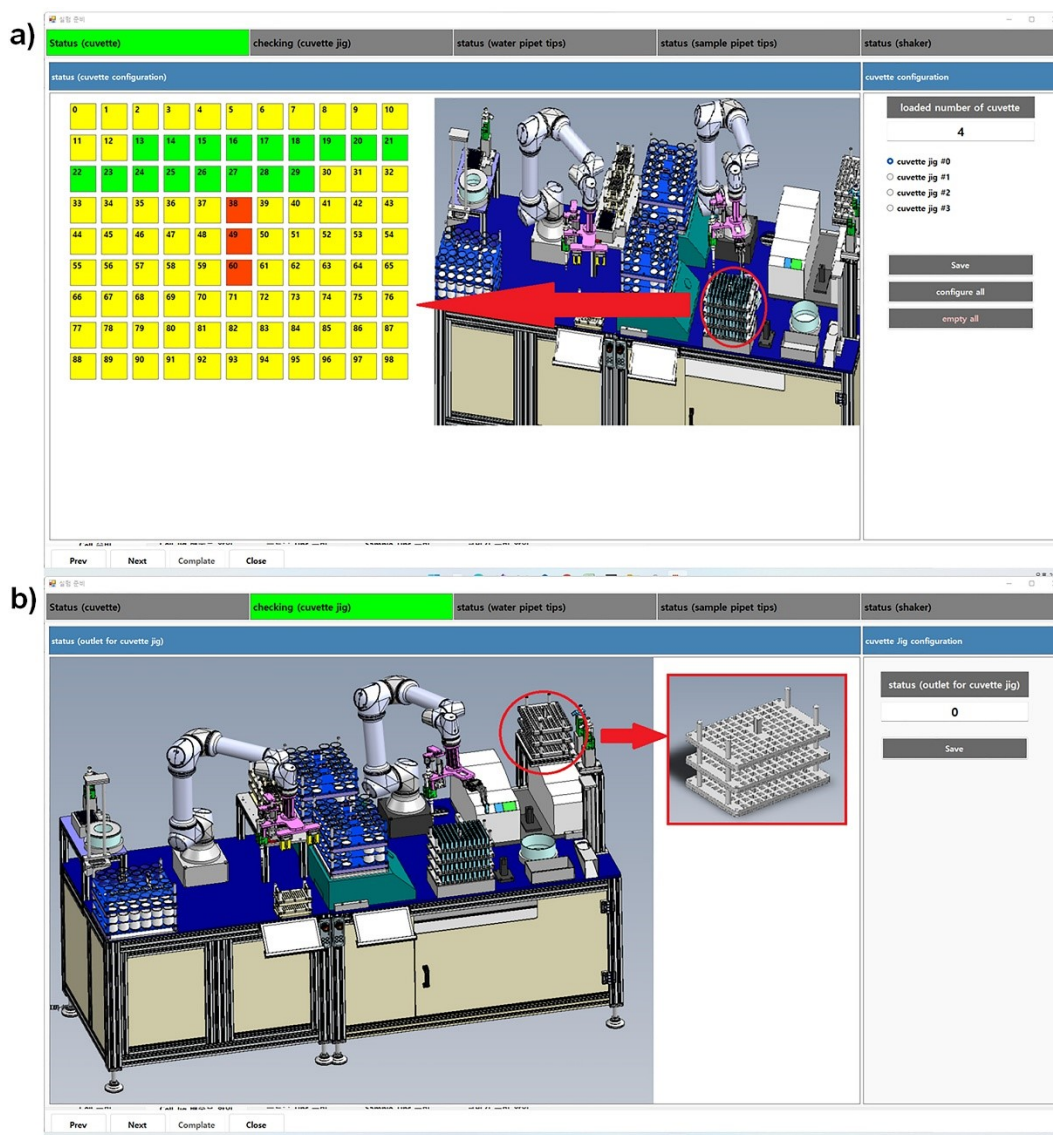


Figure S3. Graphical interface for UV-Vis cell management in the automated system used in robot program 1. (a) The interface displays the real-time status of disposable UV-Vis cells within a 96-well configuration, color-coded by usage: green for occupied cells, yellow for empty, and red for unused slots. The schematic inset shows the physical layout of the cuvette loading module as operated in robot program 1. (b) A 3D visualization highlights the cuvette outlet jig, where used cells are discarded after measurement. The right panel shows a magnified view of the outlet tray, allowing users to confirm the final disposal state. This interface is central for visualizing and validating cuvette handling during automated workflows executed by robot program 1.

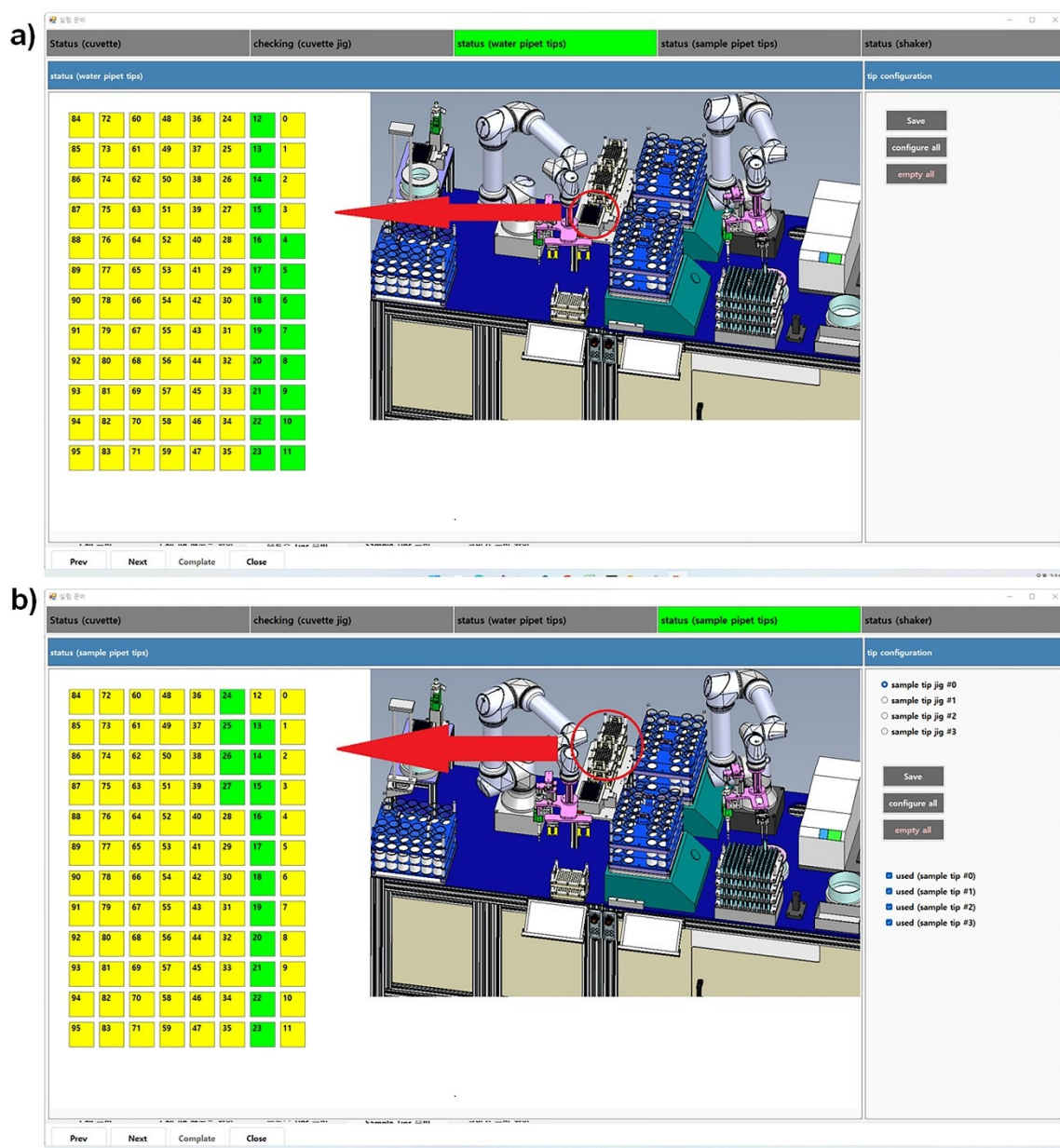


Figure S4. Pipette tip management interface for automated reagent handling in robot program 1. (a) The system monitors the status of water pipette tips using a 96-slot grid, where green indicates available tips and yellow indicates used slots. The inset highlights the physical location of the water tip tray on the robotic platform operated under robot program 1. (b) Similarly, the interface tracks sample pipette tips with real-time updates, distinguishing between filled (green) and empty (yellow) tips. The inset shows the location of the sample tip tray used for efficient sample handling during automated runs executed by robot program 1.

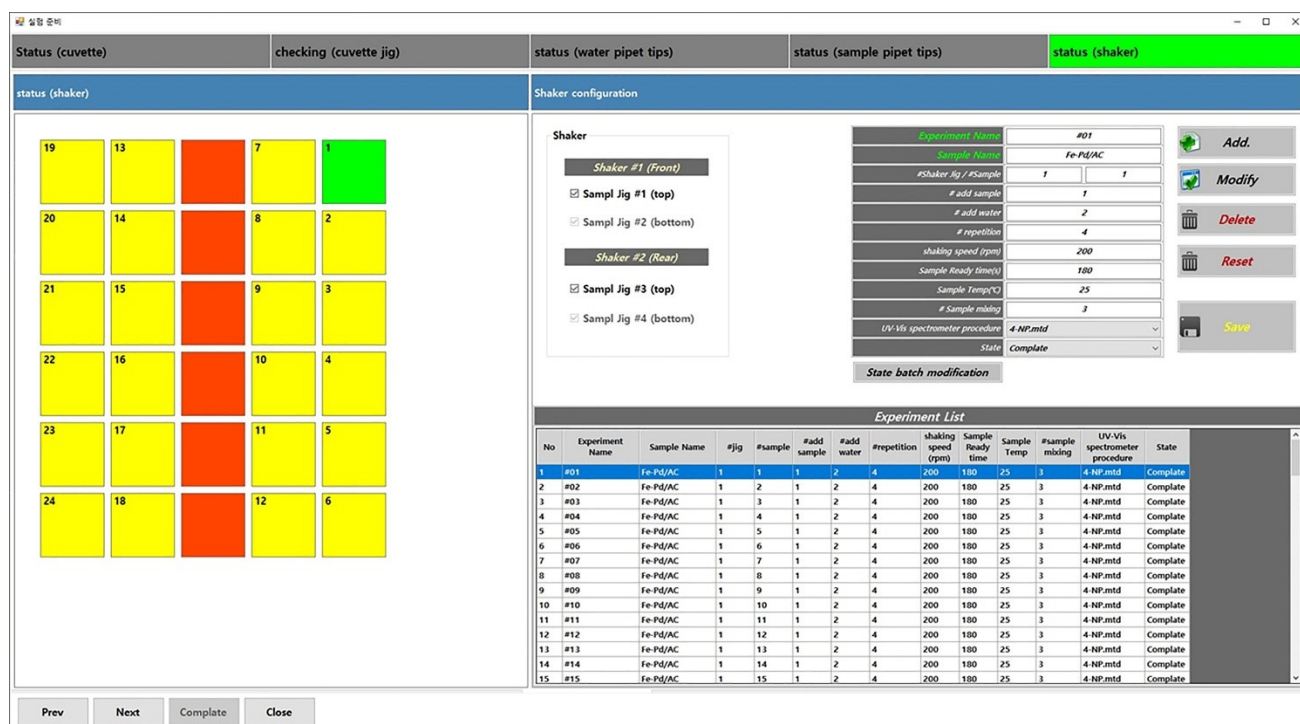


Figure S5. Shaker configuration interface for automated catalyst preparation in robot program 1. The left panel visualizes the current status of the shaker tray, with green squares indicating positions filled with disposable UV-Vis cells, yellow indicating empty cells, and red representing unused positions. The right panel displays programmable parameters for each experiment, including sample ID, jig assignment, reagent volumes, shaking speed, reaction temperature, and mixing cycles—all executed under robot program 1. The bottom panel lists completed experiments for batch tracking and state management during automated workflows controlled by robot program 1.

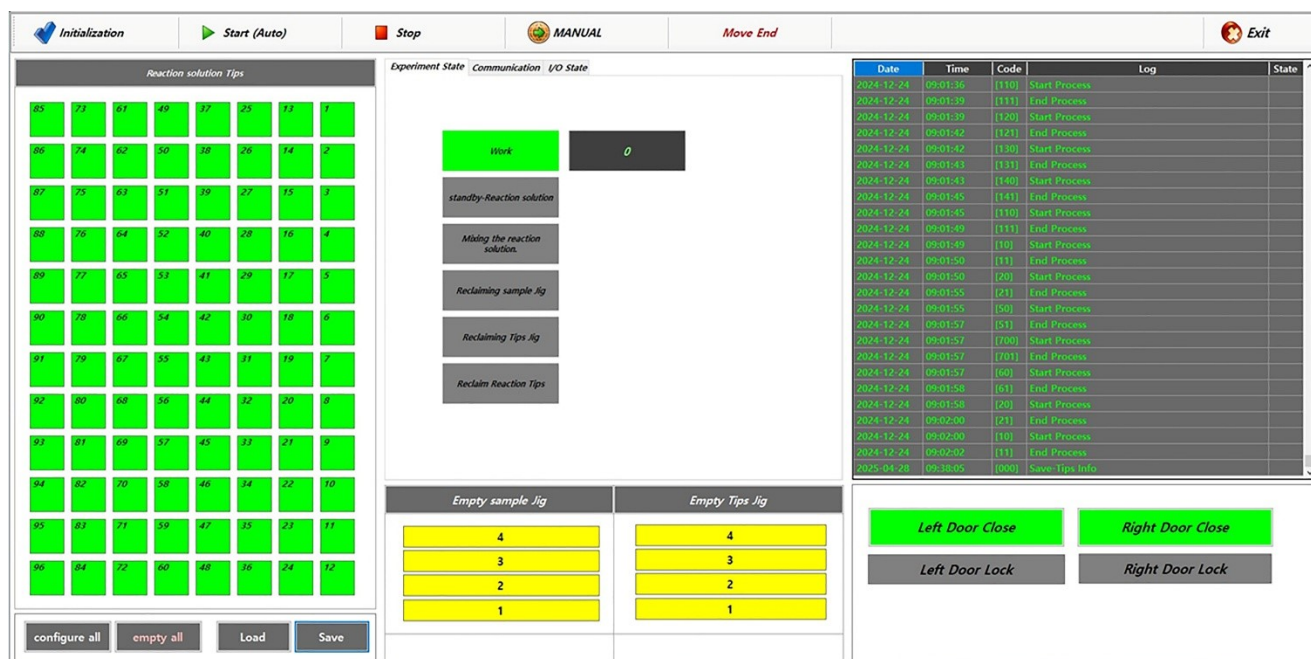


Figure S6. Status interface for reaction solution pipetting and system operations in robot program 2. The left panel shows the availability of 96 disposable pipette tips for reaction solution dispensing, with green indicating that all tips are filled and ready. The center panel tracks the current operation state such as pipetting, jig reclaim, or mixing within the workflow of robot program 2. The right panel logs each time-stamped robotic event with associated operation codes, enabling detailed diagnostics and traceability. The bottom section displays the number of available empty jigs for samples and tips, supporting efficient resource management and uninterrupted experimental execution under robot program 2.

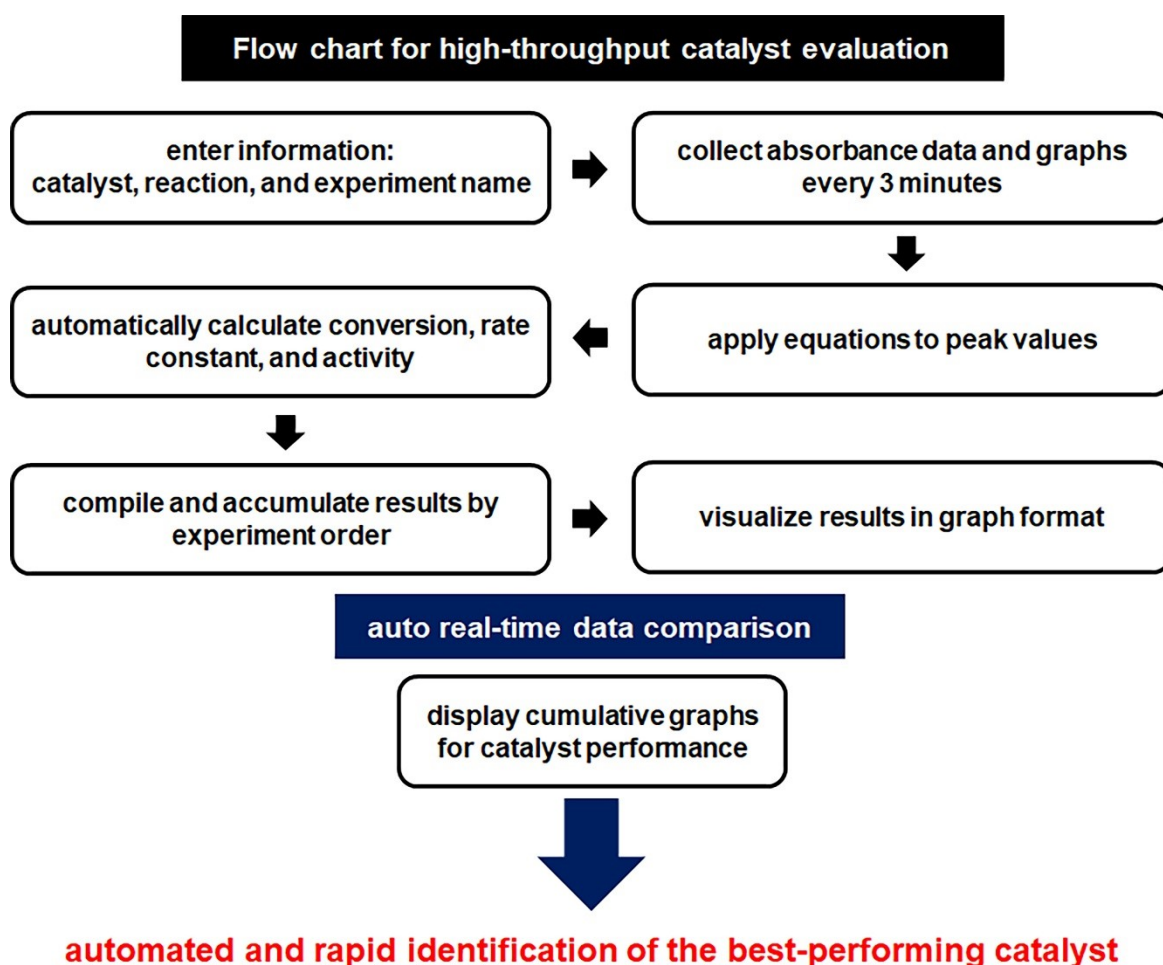


Figure S7. Flowchart of the automated high-throughput data analysis process for catalyst screening. The software workflow begins with entering basic experiment details, such as catalyst identity, reaction type, and experiment name. Absorbance data are collected every 3 min and processed using predefined equations to calculate peak values. The system then automatically determines the conversion, rate constant, and activity, compiling the results in sequential order. All outputs are visualized as graphs and compared in real time, enabling rapid and automated identification of the best-performing catalyst based on cumulative performance metrics.

Chemical Science

Information

Chemical Information					
	IUPAC name	chemical formula	weight (g)	molecular weight (g/mol)	mol
reactant	4-nitrophenol	C ₆ H ₅ NO ₃	0.01	139.11	0.000072
reductant	sodiumboro h...	NaBH ₄	0.008	37.83	0.000211
solvent	Water	H ₂ O	42	18.02	0.000072

Catalyst Information		Reaction Information	
	Information		Information
Catalyst	Pd/AC	experimental No.	#02
Active metal	Pd	used catalyst amount (g)	0.008
Support	activated char...	used reactant amount (mL)	1
Dopant		used reactant amount (mol)	7.2E-05
Atomic weight (g/mol)	106.42	rxn Temp.(°C)	25
Metal content (wt%)	10	rxn. Time (min)	9
Metal dispersion (%)	0		
Active metal (g)	0.000800		
Active metal (mol)	0.000019		

Experiment set	Experiment
Experiment set Name	Experiment Name
231213_4-NPRR	#01
231214_4-NPRR	#02
231219_4-NPRR	#03
240227_4-NPRR	#04
240308_4-NPRR(metal doping)	#05
240411_4-NPRR(metal doping)	#06
240417_4-NPRR(metal doping)	#07
4_NPRR	#08
4_NPRR(commercial Pd)	#09
	#10
	#11
	#12
	#13
	#14
	#15
	#16
	#17
	#18
	#19
	#20

Experiment set Name	Experiment Name
240417_4-NPRR(metal doping)	#02

Create Copy /Paste Delete

Load Import Save

Apply Experiment Set

Copy /Paste Delete

Figure S8. User interface for pre-input of experimental and catalyst information. The software interface enables users to enter essential chemical, catalyst, and reaction parameters before initiating automated experiments. Chemical information includes the identity, formula, mass, and molar amounts of the reactant (4-nitrophenol), reductant (NaBH₄), and solvent (DI water). Catalyst information includes metal type, support, atomic weight, metal loading, and amount of active metal. Reaction information includes catalyst and reactant quantities, reaction temperature, and time. These inputs ensure accurate kinetic calculations and reproducible catalyst evaluation results. Experiment set and individual experiment management functions are provided for streamlined batch operations.

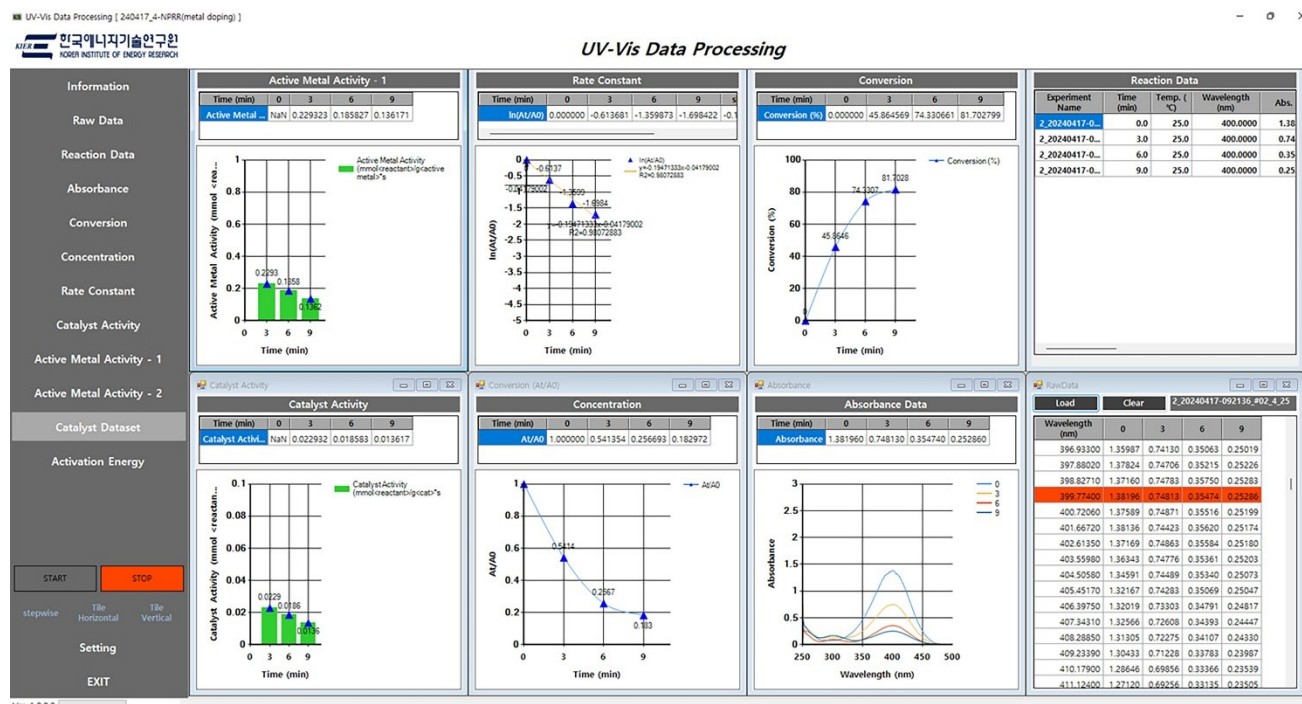


Figure S9. Screenshot of the UV-Vis data processing software used for kinetic analysis. The interface displays a comprehensive set of quantitative analyses for catalyst evaluation. Key metrics (absorbance, A_t/A_0 , conversion (%), rate constant, catalyst activity, and active metal activity) are automatically calculated and plotted based on UV-Vis spectral data collected over time.

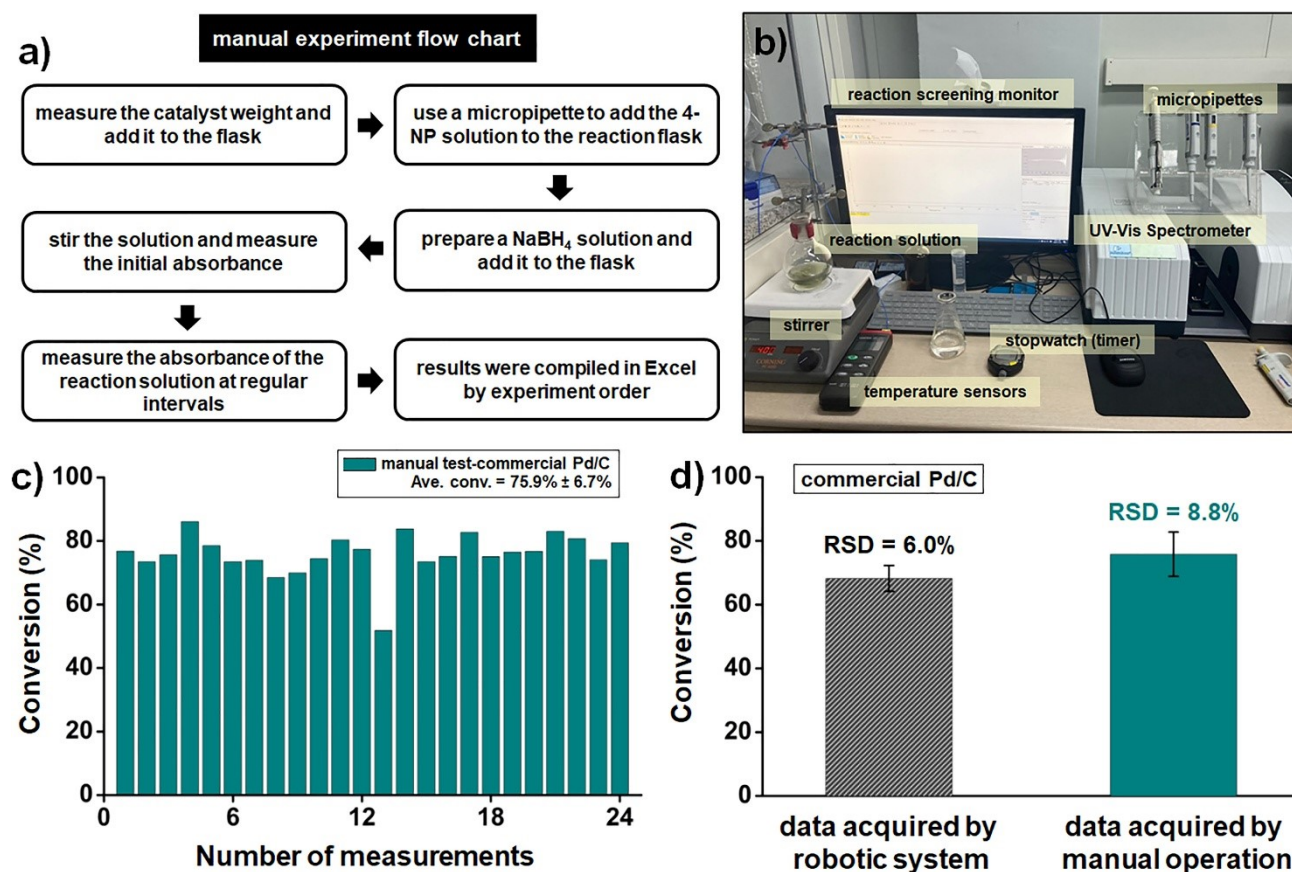


Figure S10. Comparative analysis of manual versus robotic catalyst evaluation workflows. (a) Flowchart of the manual test procedure for the reduction of 4-NP using commercial Pd/C, including catalyst weighing, reagent addition, and UV-Vis measurements at regular intervals. (b) Photograph of the manual experimental setup showing the reaction monitoring system, UV-Vis spectrometer, micropipettes, temperature sensor, and stopwatch for manual data acquisition. (c) Conversion results from 24 manually repeated experiments using commercial Pd/C. (d) Side-by-side comparison of conversion values obtained from robotic and manual operations for the same catalyst. Each data point corresponds to an independent replicate reaction ($n = 24$), carried out in separate reaction vessels prepared under identical experimental conditions.

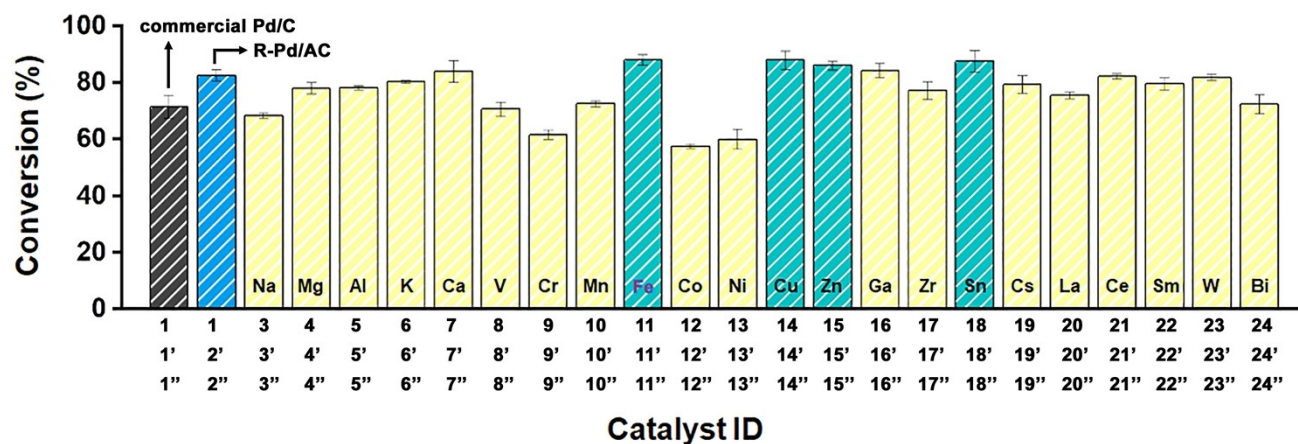


Figure S11. Conversion (%) of 24 Pd-based catalysts evaluated using the automated robotic platform. Error bars represent the standard deviation of three independent replicate experiments ($n = 3$) conducted for each catalyst.

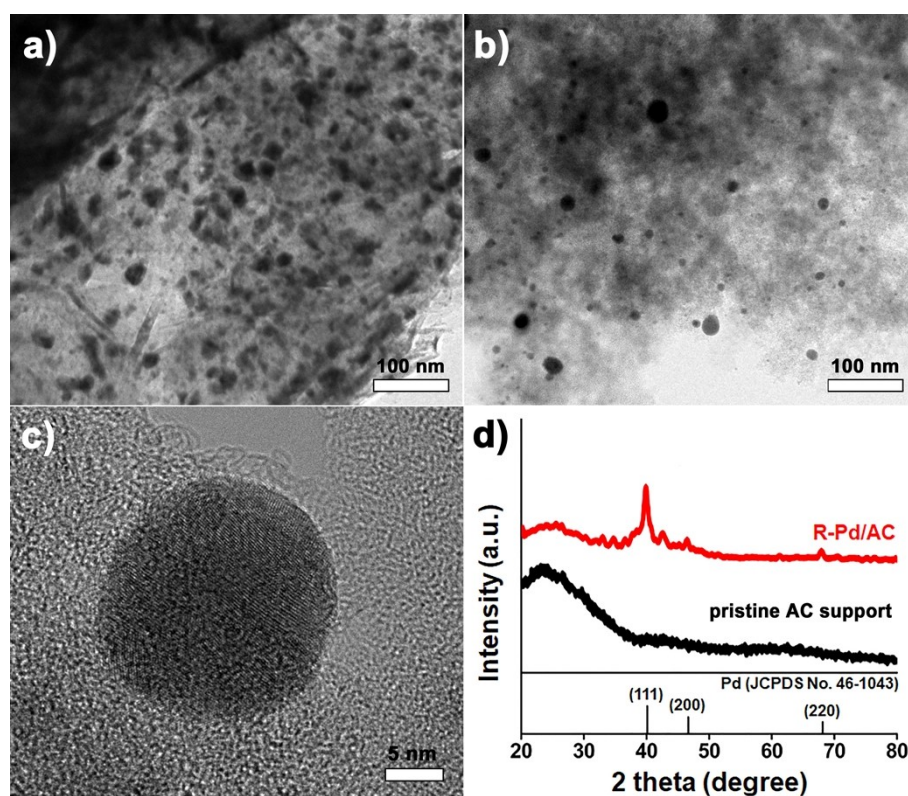


Figure S12. (a) TEM image of commercial Pd/C. (b) TEM and (c) high-resolution TEM images of the synthesized R-Pd/AC catalyst. (d) XRD patterns of R-Pd/AC compared with the pristine activated carbon support.

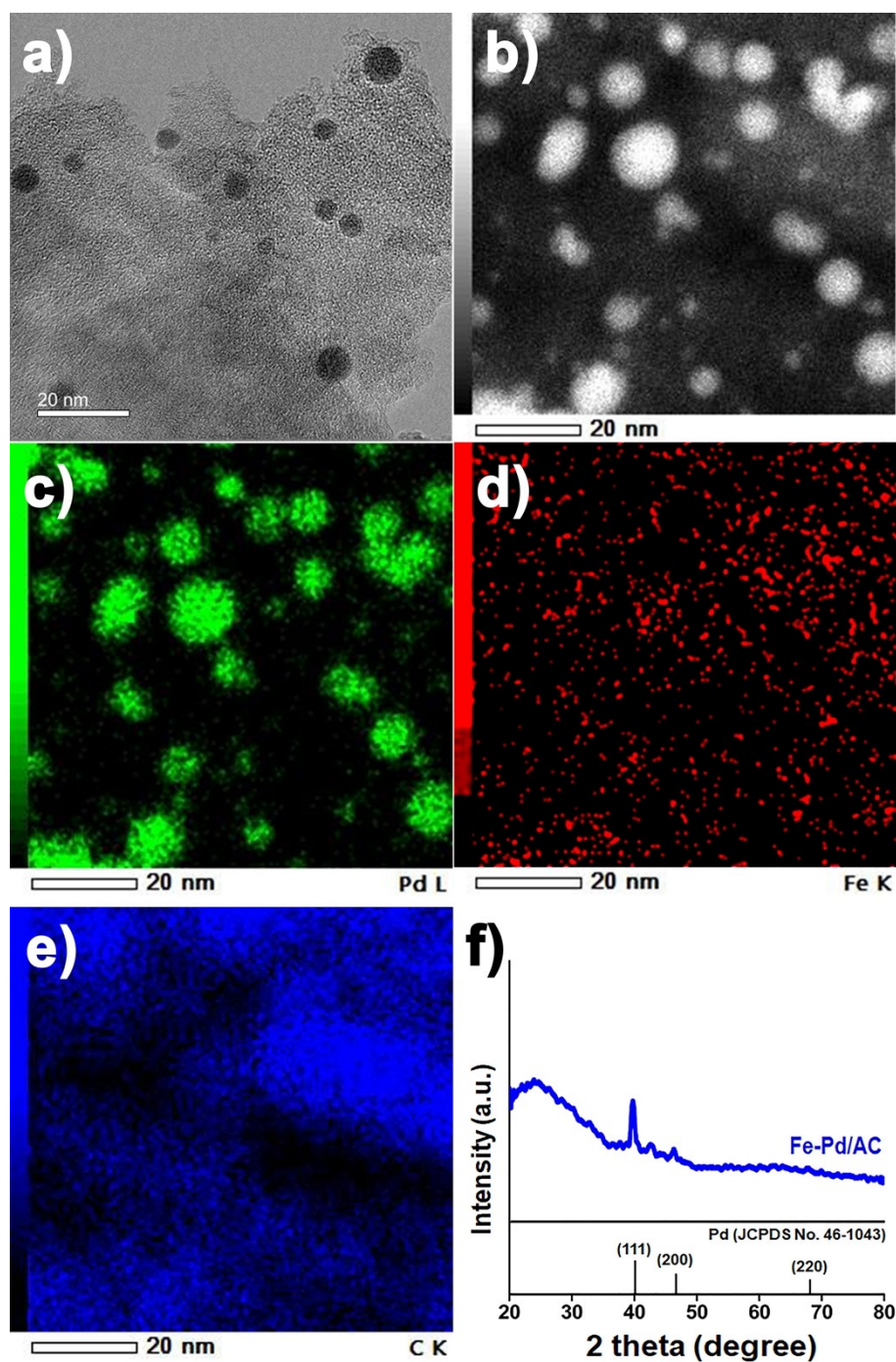


Figure S13. (a) TEM image and (b) HAADF-STEM image of Fe-Pd/AC. (c-e) Elemental mapping images: (c) Pd, (d) Fe, and (e) C. (f) XRD pattern of the Fe-Pd/AC catalyst.

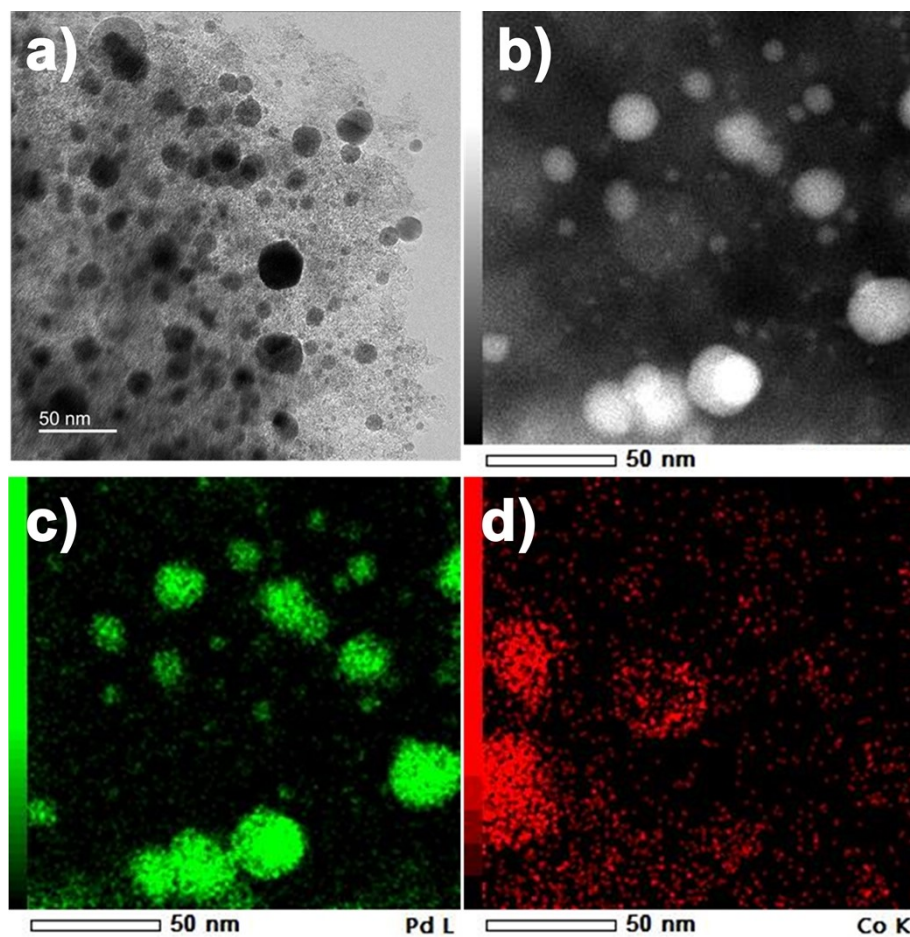


Figure S14. (a) TEM image and (b) HAADF-STEM image of Co-Pd/AC. (c-d) Elemental mapping images of the catalyst: (c) Pd and (d) Co.

Catalyst Dataset														
	Alias	Experiment Name	Time (min)	Temp. (°C)	Wavelength (nm)	Abs.	A _t /A ₀	ln(A _t /A ₀)	slope	k (s ⁻¹)	R ²	Reaction Data		
												Conversion (%)	Catalyst Activity (mmol-reactant/g-cat-h)	Active Metal Activity (mmol-reactant/g-active metal-h)
Raw Data	1	2_20240418-114-	9.0	25.0	400.0000	0.4058	0.3036	-1.1922	-0.111457	0.002191	0.98626	69.6434	0.0116	0.1161
Reaction Data	2	2_20240417-092-	9.0	25.0	400.0000	0.2529	0.1830	-1.6984	-0.194713	0.001245	0.980736	81.7028	0.0136	0.1362
	3	1_20240417-011-	9.0	25.0	400.0000	0.4716	0.3162	-1.1513	-0.130750	0.002179	0.991534	68.3164	0.0116	0.1140
	4	4_20240419-083-	9.0	25.0	400.0000	0.3803	0.2182	-1.5224	-0.172347	0.002072	0.994750	78.1811	0.0130	0.1303
	5	5_20240418-124-	9.0	25.0	400.0000	0.1282	0.2250	-1.4918	-0.164518	0.002742	0.997254	77.5033	0.0129	0.1292
Conversion	6	6_20240417-101-	9.0	25.0	400.0000	0.2790	0.1981	-1.6189	-0.181342	0.003022	0.999412	80.1880	0.0134	0.1336
Concentration	7	7_20240417-040-	9.0	25.0	400.0000	0.2847	0.1877	-1.6732	-0.186043	0.003101	0.999776	81.2349	0.0135	0.1354
	8	8_20240417-104-	9.0	25.0	400.0000	0.3941	0.2694	-1.3116	-0.143973	0.002400	0.996649	73.0619	0.0122	0.1218
	9	9_20240417-110-	9.0	25.0	400.0000	0.5332	0.3652	-0.9963	-0.111338	0.001856	0.998254	63.0795	0.0105	0.1051
	10	10_20240417-04-	9.0	25.0	400.0000	0.4080	0.2764	-1.2859	-0.141245	0.002154	0.986250	72.3596	0.0121	0.1206
Rate Constant	11	11_20240417-11-	9.0	25.0	400.0000	0.1474	0.1016	-2.2865	-0.250283	0.004171	0.993078	89.8376	0.0150	0.1497
	12	12_20240417-05-	9.0	25.0	400.0000	0.6343	0.4166	-0.8757	-0.096848	0.001614	0.999721	58.3424	0.0097	0.0972
	13	13_20240417-11-	9.0	25.0	400.0000	0.5597	0.3687	-0.9979	-0.113038	0.001884	0.996704	63.1150	0.0105	0.1052
	14	14_20240418-12-	9.0	25.0	400.0000	0.1651	0.1089	-2.2173	-0.251501	0.004182	0.995066	89.1087	0.0149	0.1485
Catalyst Activity	15	15_20240418-12-	9.0	25.0	400.0000	0.2133	0.1404	-1.9634	-0.217614	0.003627	0.998633	85.9623	0.0143	0.1433
Active Metal Activity - 1	16	16_20240418-12-	9.0	25.0	400.0000	0.2335	0.1541	-1.8701	-0.208518	0.003475	0.998866	84.5899	0.0141	0.1410
	17	17_20240418-12-	9.0	25.0	400.0000	0.3656	0.2497	-1.3874	-0.153955	0.002566	0.998597	75.0283	0.0125	0.1230
	18	18_20240418-01-	9.0	25.0	400.0000	0.1738	0.1140	-2.1720	-0.247052	0.004018	0.997998	88.6047	0.0148	0.1477
	19	19_20240418-04-	9.0	25.0	400.0000	0.2907	0.1881	-1.6707	-0.157677	0.003128	0.996886	81.1879	0.0135	0.1353
Active Metal Activity - 2	20	20_20240418-10-	9.0	25.0	400.0000	0.3665	0.2589	-1.3554	-0.151275	0.002521	0.980491	74.1324	0.0124	0.1235
	21	21_20240418-04-	9.0	25.0	400.0000	0.2741	0.1789	-1.7209	-0.194072	0.003235	0.996764	82.1094	0.0137	0.1368
	22	22_20240418-05-	9.0	25.0	400.0000	0.2921	0.1812	-1.7080	-0.188148	0.003136	0.999292	81.8776	0.0136	0.1365
	23	23_20240418-05-	9.0	25.0	400.0000	0.2714	0.1736	-1.7508	-0.195792	0.003263	0.999340	82.6369	0.0138	0.1377
	24	24_20240417-08-	9.0	25.0	400.0000	0.5234	0.3083	-1.1756	-0.124214	0.002137	0.994793	69.1712	0.0115	0.1153

Figure S15. Data summary table generated by the automated UV-Vis data processing software. The dataset includes 24 catalyst experiments with key reaction metrics: absorbance (Abs.), concentration ratio (A_t/A_0), natural logarithm of the concentration ratio ($\ln(A_t/A_0)$), linear regression slope, pseudo-first-order rate constant (k), regression coefficient (R^2), and conversion efficiency (%). Calculated values for catalyst activity and active metal activity are also provided for quantitative comparison among catalyst samples.

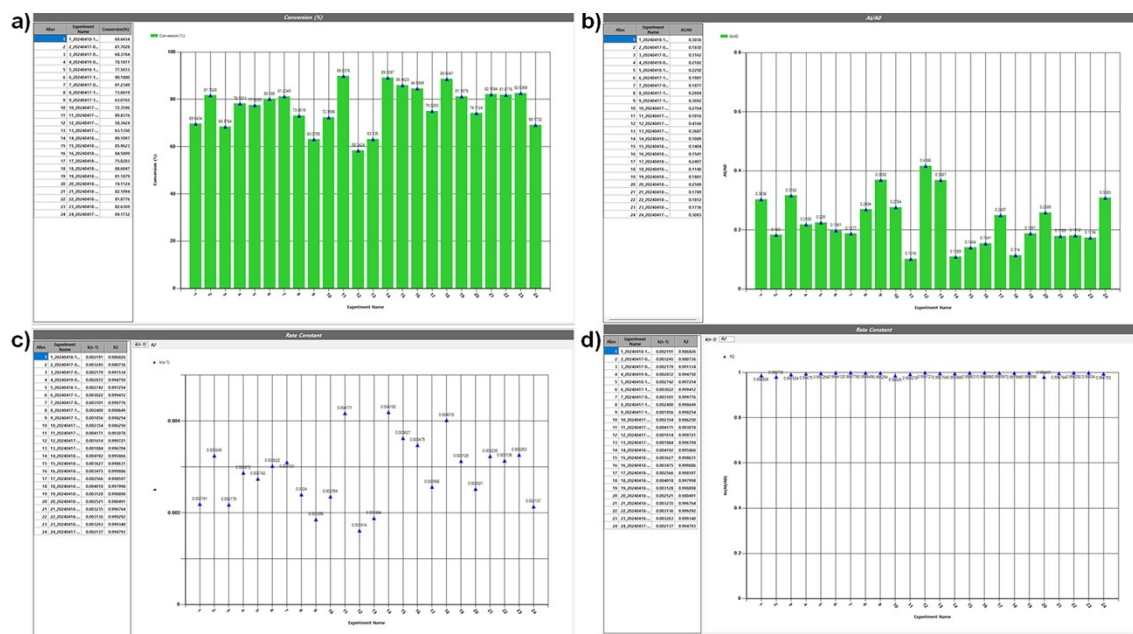


Figure S16. Real-time visualization of kinetic metrics automatically generated from the 24-sample catalyst screening. (a) Conversion (%) profile of 24 selected experiments at the 9 min mark, showing consistent catalytic performance for Fe-Pd/AC. (b) A_t/A_0 values confirming the extent of reaction progress. (c) Pseudo-first-order rate constants (k) calculated from linear fitting of $\ln(A_t/A_0)$ versus time. (d) R^2 values for kinetic fitting.

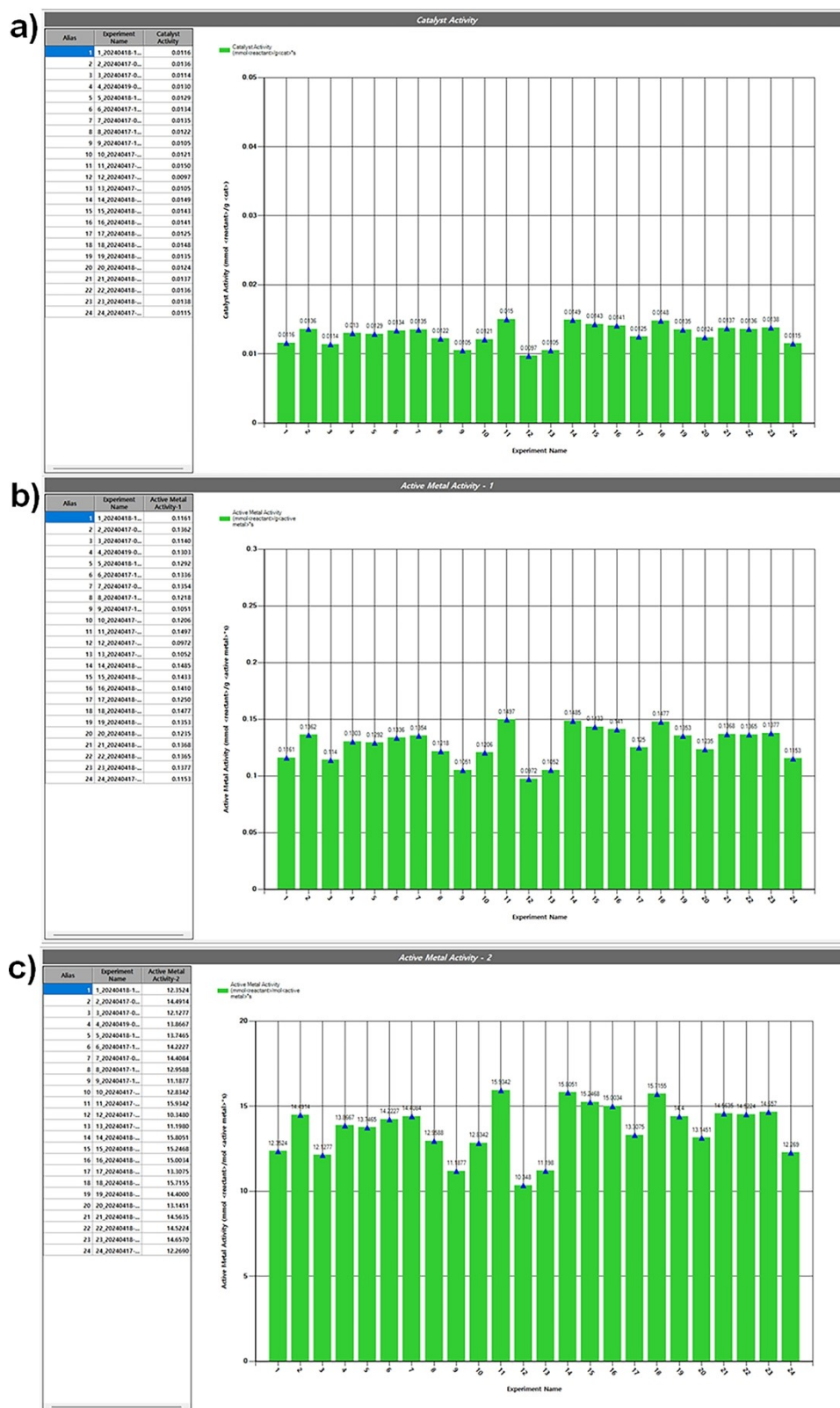


Figure S17. Quantitative analysis of catalytic activity and normalized performance metrics for 24 catalyst samples. (a) Catalyst activity calculated as mmol of reactant converted per gram of catalyst per minute. (b) Active metal activity normalized by the weight of active Pd metal ($\text{mmol} \cdot \text{g}_{\text{Pd}}^{-1} \cdot \text{min}^{-1}$). (c) Active metal activity normalized by the molar amount of Pd ($\text{mmol} \cdot \text{mol}_{\text{Pd}}^{-1} \cdot \text{min}^{-1}$).

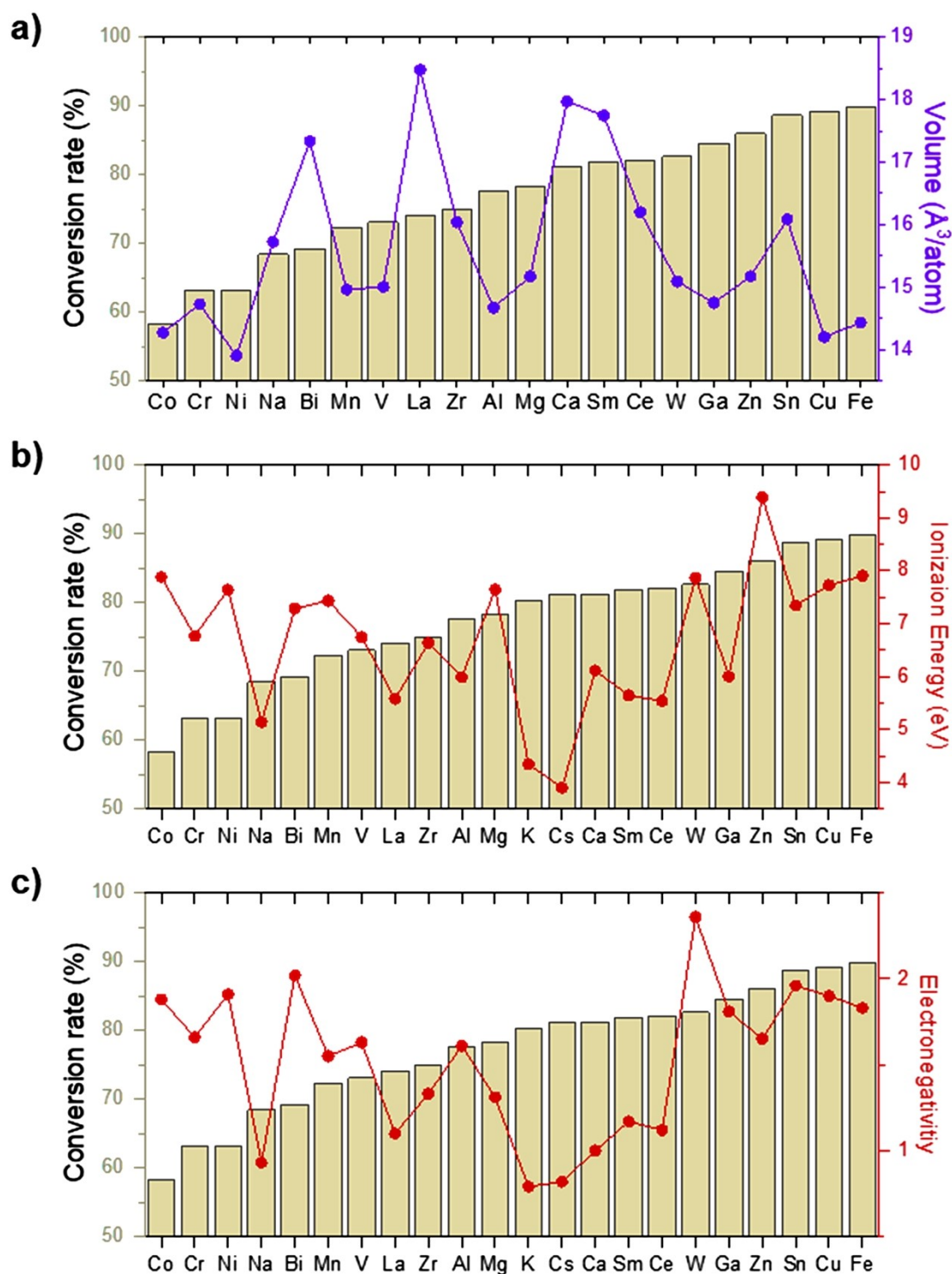


Figure S18. (a) Volume per atom of M-Pd alloys, (b) ionization energy, and (c) electronegativity (Pauling) of the M metals, plotted in order of increasing M-Pd/AC conversion rate, shown as background bars.

Table S1. Catalyst compositions and additive precursor information for 22 M-Pd/AC nanocatalysts.*

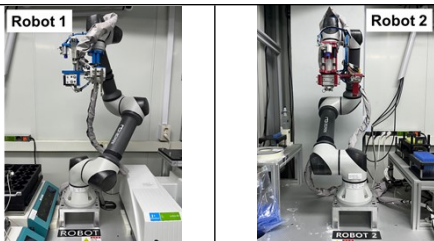
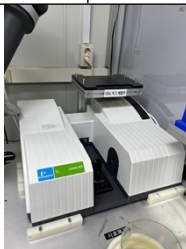


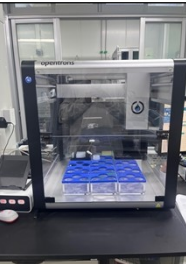

No.	Additive precursor	Chemical formula	Additive metal	Catalyst
1	Sodium hydroxide	NaOH	Na	Na-Pd/AC
2	Magnesium(II) nitrate hexahydrate	$\text{Mg}(\text{NO}_3)_2 \cdot 6\text{H}_2\text{O}$	Mg	Mg-Pd/AC
3	Aluminum(III) nitrate nonahydrate	$\text{Al}(\text{NO}_3)_3 \cdot 9\text{H}_2\text{O}$	Al	Al-Pd/AC
4	Potassium hydroxide	KOH	K	K-Pd/AC
5	Calcium chloride dihydrate	$\text{CaCl}_2 \cdot 2\text{H}_2\text{O}$	Ca	Ca-Pd/AC
6	Vanadium(III) chloride	VCl_3	V	V-Pd/AC
7	Chromium(III) nitrate nonahydrate	$\text{Cr}(\text{NO}_3)_3 \cdot 9\text{H}_2\text{O}$	Cr	Cr-Pd/AC
8	Manganese(II) chloride tetrahydrate	$\text{MnCl}_2 \cdot 4\text{H}_2\text{O}$	Mn	Mn-Pd/AC
9	Iron(II) acetate	$\text{Fe}(\text{CH}_3\text{COO})_2$	Fe	Fe-Pd/AC
10	Cobalt(II) acetate tetrahydrate	$\text{Co}(\text{CH}_3\text{COO})_2 \cdot 4\text{H}_2\text{O}$	Co	Co-Pd/AC
11	Nickel(II) chloride hexahydrate	$\text{NiCl}_2 \cdot 6\text{H}_2\text{O}$	Ni	Ni-Pd/AC
12	Copper(II) chloride dihydrate	$\text{CuCl}_2 \cdot 2\text{H}_2\text{O}$	Cu	Cu-Pd/AC
13	Zinc nitrate hexahydrate	$\text{Zn}(\text{NO}_3)_2 \cdot 6\text{H}_2\text{O}$	Zn	Zn-Pd/AC
14	Gallium(III) nitrate hydrate	$\text{Ga}(\text{NO}_3)_3 \cdot x\text{H}_2\text{O}$	Ga	Ga-Pd/AC
15	Zirconium(IV) chloride (anhydrous)	ZrCl_4	Zr	Zr-Pd/AC
16	Tin(II) chloride	SnCl_2	Sn	Sn-Pd/AC
17	Cesium carbonate	Cs_2CO_3	Cs	Cs-Pd/AC
18	Lanthanum(III) nitrate hexahydrate	$\text{La}(\text{NO}_3)_3 \cdot 6\text{H}_2\text{O}$	La	La-Pd/AC
19	Cerium(III) nitrate hexahydrate	$\text{Ce}(\text{NO}_3)_3 \cdot 6\text{H}_2\text{O}$	Ce	Ce-Pd/AC
20	Samarium(III) nitrate hexahydrate	$\text{Sm}(\text{NO}_3)_3 \cdot 6\text{H}_2\text{O}$	Sm	Sm-Pd/AC
21	Tungstic acid	H_2WO_4	W	W-Pd/AC
22	Bismuth(III) nitrate pentahydrate	$\text{Bi}(\text{NO}_3)_3 \cdot 5\text{H}_2\text{O}$	Bi	Bi-Pd/AC

*All metal promoters were added at a fixed 10 mol % relative to the moles of Pd in the Pd/AC catalyst. This ratio was maintained consistently across all wet-impregnation procedures to ensure uniform metal loading conditions and allow direct comparison of promoter effects.



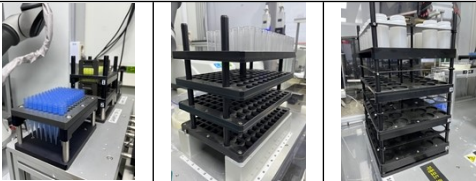

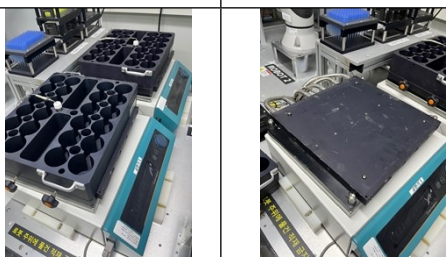
Table S2. The calculated material properties of the M-Pd binary and M unary systems extracted from the Materials Project database. (E_f : formation energy, ϵ_d : d -band center, Φ : work function, I.E. : ionization energy, EN : electronegativity (Pauling)).

M	M-Pd MP-id	M Ratio	E_f (eV/atom)	Volume (Å ³ /atom)	ϵ_d (eV)	M MP-id	Φ (eV)	I.E.	EN
Na	976971	0.250	0.000	15.723	0.907	10172	2.654	5.1391	0.93
Mg	976976	0.167	-0.332	15.169	-0.804	153	3.552	7.6462	1.31
Al	605663	0.167	-0.462	14.672	-0.508	134	4.037	5.9858	1.61
K	1180861	0.667	0.132	39.238	6.341	972981	2.108	4.3407	0.82
Ca	11826	0.167	-0.366	17.971	-0.602	45	2.774	6.1132	1
V	1216296	0.200	-0.157	15.003	0.873	146	4.110	6.7462	1.63
Cr	865786	0.250	-0.127	14.726	0.233	90	4.107	6.7665	1.66
Mn	31138	0.250	-0.229	14.959	0.340	35	4.320	7.434	1.55
Fe	21845	0.250	-0.108	14.429	-0.681	13	4.310	7.9024	1.83
Co	1183687	0.250	0.002	14.271	0.398	102	4.855	7.881	1.88
Ni	973983	0.250	0.068	13.902	-0.156	23	4.980	7.6398	1.91
Cu	1184119	0.250	-0.051	14.202	0.267	30	4.534	7.7264	1.9
Zn	1215579	0.200	-0.231	15.174	0.231	79	4.006	9.3942	1.65
Ga	1184278	0.250	-0.443	14.749	-3.019	142	4.081	5.9993	1.81
Zr	30842	0.250	-0.852	16.041	0.014	131	3.571	6.6339	1.33
Sn	718	0.250	-0.493	16.085	-2.647	117	4.072	7.3439	1.96
Cs	-	-	-	-	-	1	2.033	3.8939	0.79
La	30753	0.167	-0.597	18.479	-1.660	26	2.635	5.5769	1.1
Ce	1025415	0.125	-0.485	16.199	-0.094	28	2.977	5.5387	1.12
Sm	357	0.250	-0.854	17.747	0.031	69	2.741	5.6437	1.17
W	1219940	0.200	0.007	15.091	0.778	91	4.469	7.864	2.36
Bi	30463	0.250	-0.233	17.334	0.764	23152	4.060	7.2856	2.02

Table S3. Components of the robotic system, including commercial instruments and custom-designed parts, with manufacturer and model information.

Component	Description	Manufacturer/ Model	Photograph
Robotic arm	6-axis collaborative robot	Rainbow Robotics/ RB5-850	
UV-Vis spectrometer	190-1100 nm spectral range with dual deuterium and tungsten-halogen light sources, capable of full-spectrum acquisition within ~20 ms using PDA technology	PerkinElmer/ Lambda 465	
Peristaltic pump	Water transfer	Labscitech/ LEPP600F+Y T15	
Auxiliary robot	Pump-hose manipulation and transport	Wlkata/ Mirobot	
Liquid-handling robot	Automated dispensing of small-volume liquids	Opentrons/ OT-2	
Shaker	For homogenizing reaction solutions by shaking the reaction vessels	Jeiotech/ OS-2000	

Chemical Science

Cuvettes	Disposable polypropylene cuvettes for UV-Vis measurements (1 cm optical pathlength)	Kartell/ KA.1939	
Thermal controller	Heating-block temperature control unit	HanYoungNu x/ NX4-04	
Jig components	Racks for cuvette, reaction vessels, pipette tips	Custom-designed	
Gripper	Versatile gripper for cuvette transport, pipetting operations, and jig replacement	Custom-designed	
Detachable heating plate and heating block	Reaction temperature control	Custom-designed	

Movie S1. Conceptual 3D animation illustrating the operation of the automated robotic platform.

Movie S2. Main actions for jig handling by robot 1 and robot 2.

Movie S3. Integrated screen recording of the real-time data processing software and CCTV footage of the robotic evaluation system during unattended operation.

Movie S4. Video showing the operation of the automated pipetting device.

Movie S5. Demonstration video of the automated liquid dispensing module.